SF2A 2015
F. Martins, S. Boissier, V. Buat, L. Cambrésy and P. Petit (eds)

TRAPPING PROTOPLANETS AT THE SNOWLINES.

K. Baillié[1,2], S. Charnoz[1,2] and E. Pantin[2]

Abstract. We follow the viscous evolution of protoplanetary disks by modeling self-consistently their dynamics, thermodynamics, photosphere geometry and composition (Baillié & Charnoz., 2014, ApJ and Baillié et al., 2015, A&A). Our hydrodynamical numerical code allows us to estimate the local gradients in temperature and density that drive the type I migration of planetary embryos. In particular, we identify irregular structures in the disk: shadowed regions that are not directly irradiated by the star, temperature plateaux at the sublimation temperature of the main dust components of the disk. These icelines appear to be related with planetary traps. Though planetary embryos can be trapped temporarily in some early transient traps, the other traps (more permanent) will allow protoplanets to survive and favor their growth by collisions between embryos at some specific orbits.

Keywords: Protoplanetary disks, Planets and satellites: formation, Planet-disk interactions, Accretion disks, Planets and satellites: dynamical evolution and stability, Hydrodynamics

1 Introduction

Numerical simulations from Baillié & Charnoz (2014) and Baillié et al. (2015) were able to retrieve observational constraints on surface mass density and geometrical profiles of protoplanetary disks. Their viscous spreading hydrodynamical code involves coupling the photosphere geometry, the disk thermodynamics, its dynamics and the disk composition (through a thorough opacity model based on Helling et al. (2000); Semenov et al. (2003)). In the present work, we estimate the impact of realistic disk profiles on protoplanet migration: we identify favorable locations for planet traps and deserts. We then vary the planet radius and mass to build migration maps showing how planet traps are migrating and surviving along the disk evolution.

2 Model

2.1 Dynamical and thermodynamical evolution

The present numerical model is based on the hydrodynamical code described in Baillié & Charnoz (2014); Baillié et al. (2015), following the viscous evolution of a viscous α disk (Shakura & Sunyaev 1973). Most of the usual asumptions are removed: we follow the disk evolution from an already formed Minimum Mass Solar Nebula and not just its final steady state. We jointly calculate the photosphere geometry: the angle at which the photosphere sees the star is governing the amount of energy that the photosphere is receiving from the star. Therefore, the disk is not only heated by viscous heating but also by stellar irradiation. The iterative process calculating the temperature also calculates a consistent photosphere height, therefore coupling the disk geometry with the disk thermodynamics, which is also linked to the dynamical evolution through the viscosity, as detailed in Equation 2.1 (Lynden-Bell & Pringle 1974) obtained from the mass and angular momentum conservation.

$$\frac{\partial \Sigma(r,t)}{\partial t} = \frac{3}{r}\frac{\partial}{\partial r}\left(\sqrt{r}\,\frac{\partial}{\partial r}\left(\nu(r,t)\,\Sigma(r,t)\,\sqrt{r}\right)\right) \tag{2.1}$$

[1] IPGP / Université Paris Diderot, Paris, France
[2] AIM / CEA, Paris, France

Elements	Sublimation Temperature	Relative Abundances
Water ice	160 K	59.46 %
Volatile Organics	275 K	5.93 %
Refractory Organics	425 K	23.20 %
Troilite (FeS)	680 K	1.57 %
Olivine	1500 K	7.46 %
Pyroxene	1500 K	2.23 %
Iron	1500 K	0.16 %

Table 1. Sublimation temperatures and relative abundances that affect the disk gas opacity.

2.2 Opacity model

The main elements of the disk dust are listed in Table 1 with their sublimation temperatures. As the midplane temperature varies accross the protoplanetary disk, the physical phases of the various elements change as well. This affects the disk opacity which in turn affects the temperature. Therefore, we tabulate the dust opacity as a function of the temperature and we use this updated local opacity in our iterative process for the determination of the temperature and geometry. We use the tabulated values from Helling et al. (2000); Semenov et al. (2003) summarized in Figure 1.

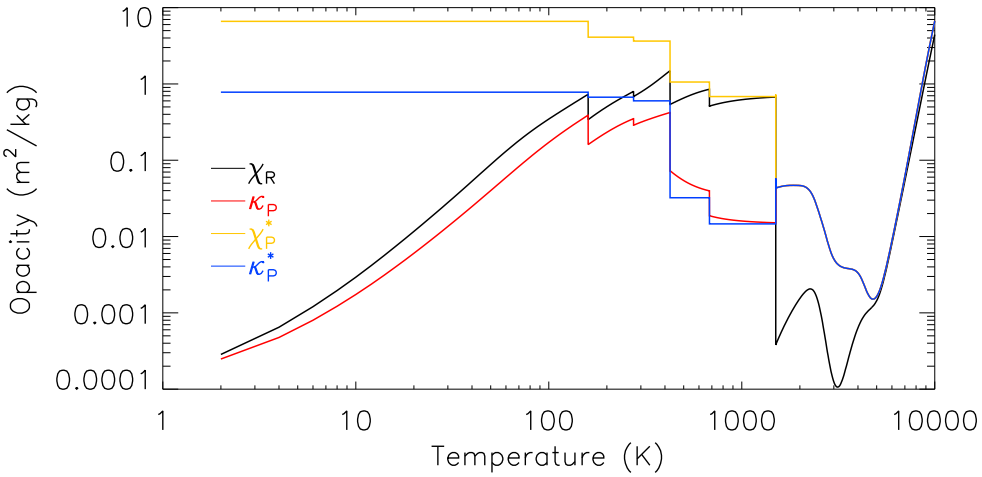

Fig. 1. Opacity variations with local temperature. Black: Rosseland mean opacity in extinction. Red: Planck mean opacity in absorption. Yellow: Planck mean opacity in extinction at stellar irradiation temperature. Blue: Planck mean opacity in absorption at stellar irradiation temperature.

The various opacities show very abrupt drops around the sulbimation temperatures of the dust elements.

3 Impact of the disk evolution on planet migration

An already formed planetary embryo exchanges angular momentum with the disk (Goldreich & Tremaine 1979, 1980) due to the resonances excited by the planet in the disk. The planet exerts a torque on the disk and therefore the disk exerts an opposite torque on the planet. We assume that the disk structure is not modified by the presence of the planet.

3.1 Lindblad torques

Using a two-dimensional approximation, considering laminar disks, a planet on a circular orbit, ignoring the disk self-gravity and assuming thermal equilibrium, Paardekooper & Papaloizou (2008) were able to derive the following formula for the total Lindblad torque exerted by the disk over the planet:

$$\Gamma_{\rm Lindblad} = -\frac{\Gamma_0(r_P)}{\gamma}\left(2.5 - 1.7\frac{\partial \ln T}{\partial \ln r}(r_P) + 0.1\frac{\partial \ln \Sigma}{\partial \ln r}(r_P)\right), \tag{3.1}$$

with $\gamma = 1.4$, the adiabatic index,
$\Gamma_0(r_P) = \left(\frac{q}{h}\right)^2 \Sigma(r_P)\, r_P^4\, (\Omega(r_P))^2$,
$h = \frac{h_{\rm press}(r_P)}{r_P}$,
and $\Omega(r_P)$ the Keplerian angular velocity at the planet position in the disk.

3.2 Corotation torques

Corotation resonances are known to exert complicated torques that include linear and nonlinear parts. Paardekooper & Papaloizou (2009b) showed that the corotation torques are generally nonlinear in the usual range of viscosity ($\alpha_{\rm visc} < 0.1$). The nonlinear contribution, due to the horseshoe drag (Ward 1991) caused by the interaction between the planet and the fluid element moving in its vicinity, is also known for having two possible origins: barotropic, intially formalized by Tanaka et al. (2002), and entropic, detailed by Baruteau & Masset (2008).

Concerning the horseshoe drag, Paardekooper et al. (2011) described the density perturbation generated by the corotation resonances and provided expressions for both the entropy and vortensity (or barotropic) contributions. Assuming a gravitational softening $b = 0.4h_{\rm press}$, Bitsch & Kley (2011) and Bitsch et al. (2014) summarized these expressions to obtain the following contributing torques:

$$\Gamma_{\rm hs,entro} = -\frac{\Gamma_0(r_P)}{\gamma^2}\, 7.9\left(-\frac{\partial \ln T}{\partial \ln r}(r_P) + (\gamma-1)\frac{\partial \ln \Sigma}{\partial \ln r}(r_P)\right) \tag{3.2}$$

$$\Gamma_{\rm hs,baro} = -\frac{\Gamma_0(r_P)}{\gamma} 1.1\left(\frac{\partial \ln \Sigma}{\partial \ln r}(r_P) + \frac{3}{2}\right) \tag{3.3}$$

It appears that this unsaturated corotation torque strongly depends on the temperature and surface mass density gradients. It also scales with $M_{\rm P}^2$, as does the Lindblad torque. However, Paardekooper & Papaloizou (2009a) showed that given the viscous, diffusive, and libration timescales, the linear effects of the corotation torques can be saturated for some viscosities and some planet masses. For our disk that evolved for 1 Myr, the viscosity range compared to Fig. 14 from Paardekooper & Papaloizou (2009a) suggests that saturation cannot be neglected for planetary masses higher than $6M_\oplus$. Paardekooper et al. (2011) defined weight functions for the partial saturation of the corotation torque. These functions vary with the half-width of the horseshoe, which depends on the mass of the planet. Appendix A of Bitsch & Kley (2011) summarized this method and added correcting factors. We used a similar torque calculation, which is necessary to take into account the variations with the planet mass.

3.3 Planet migration

The total torque exerted by the disk on the planet is then given by $\Gamma_{\rm tot} = \Gamma_{\rm Lindblad} + \Gamma_{\rm hs,entro} + \Gamma_{\rm hs,baro}$. This total torque strongly depends on the temperature and surface mass density gradients.

Figure 2 shows a snapshot of the disk profile after 1 million years of evolution: evolved surface mass density and temperature profiles are displayed along with the total torque exerted by the disk on a planet located at a given radial distance r from the star after 1 million years of evolution of the protoplanetary disk.

The regions of negative torques are the regions in which planets will migrate inward while they would migrate outward in the regions of positive total torque. Therefore, we can identify lines of divergence that are going to be depleted in planetary embryos (planet deserts) and lines of convergence where planets will accumulate (planet traps). Traps are very important for two reasons: first they prevent protoplanets from falling onto their host star by inward migration; secondly, they favor accumulation of embryos and therefore their collisions and growth by accretion.

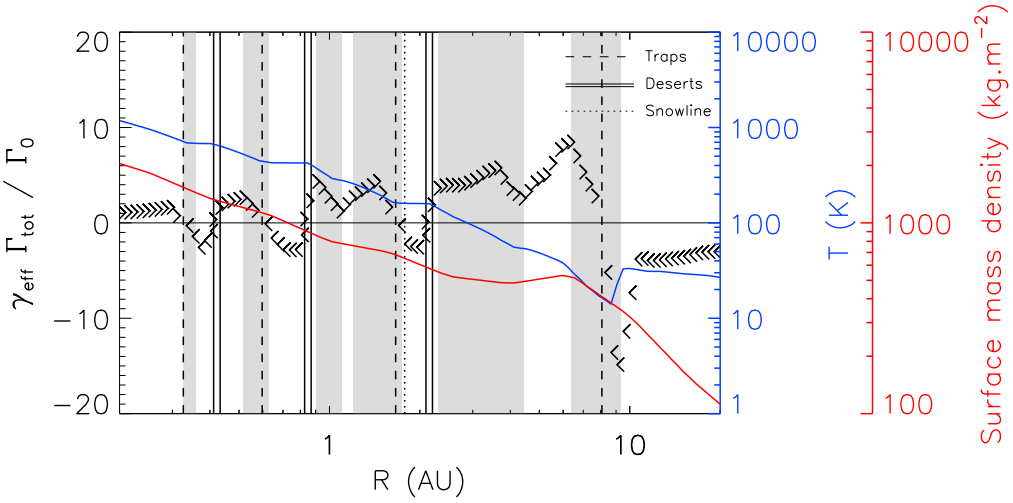

Fig. 2. Total torque exerted by a 1 million-year evolved disk on a 10-$M_{\rm Earth}$ planet versus planet radius. The surface mass density profile appears in red and the temperature profile in blue. Shadowed regions are displayed in gray.

3.4 Evolution of planetary traps and deserts

Figure 3 shows the time evolution of traps and deserts locations. These positions appears to relate quite well with the sublimation lines of the main dust components. In addition, the irradiation-viscous heating barrier seems to generate a population of planet traps that appears to be quite sustainable. Other, more transient trap populations disappear quite early in the disk evolution.

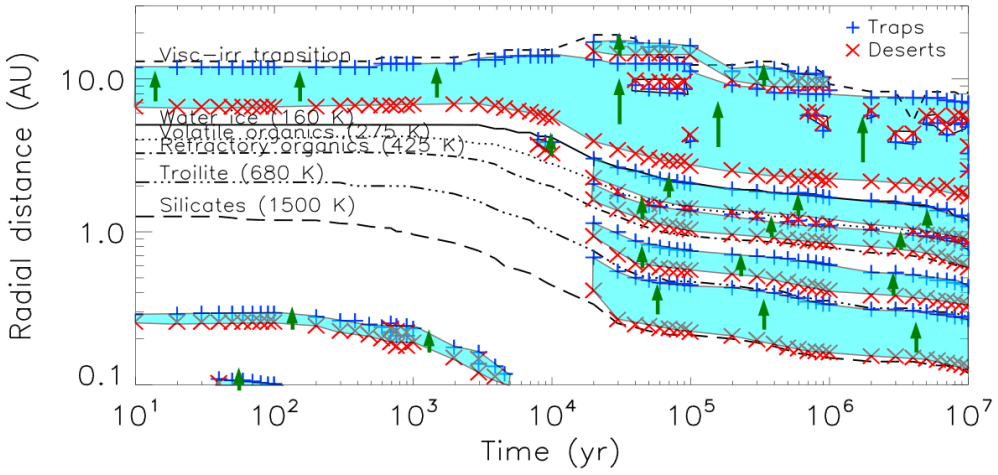

Fig. 3. Time evolution of the locations of planetary traps and deserts for a 10 Earth-masses planet.

Figure 4 displays how the total torque exerted by the disk on the planet depends on the planet mass. It shows islands of outward migration which have planet traps at their outer edge and deserts at their inner edge. As they grow in mass, planet will follow these island borders vertically and will maybe jump from one trap to the inner one as they grow. This work is being investigated currently.

4 Conclusions and perspectives

The proper consideration of the disk composition and the sublimation of the dust main components generates temperature gradient irregularities that could significantly affect the migration torques exerted by the disk on

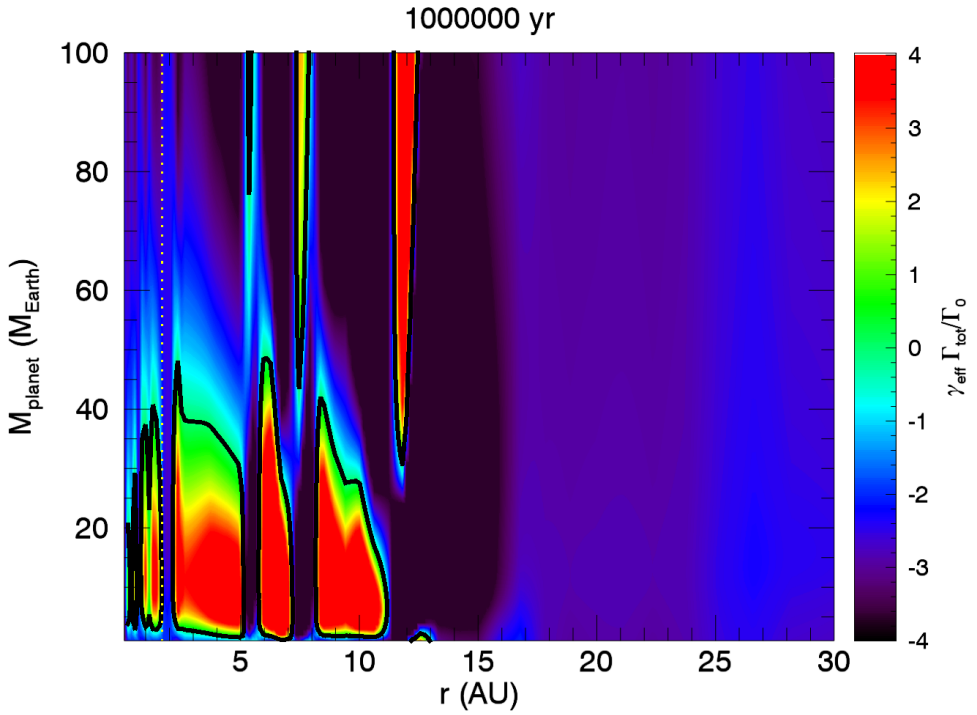

Fig. 4. Total torque exerted by the disk after 1 million year of evolution on a planet versus its radius and mass.

a putative planet. With these refinements, it appears possible to actually trap planets at a specific radius, or to clear a specific position of all planetary embryos. After 1 Myr, we identify several planetary traps and deserts below 10 AU. Most planet traps appear to be related to viscous-irradiation frontier and sublimation lines. They appear early enough in the disk evolution to help protoplanet survive planetary migration and favor their growth by collisions/accretion.

This work was supported by IDEX Sorbonne Paris Cité. We acknowledge the financial support from the UnivEarthS Labex program of Sorbonne Paris Cité (ANR-10-LABX-0023 and ANR-11-IDEX-0005-02).

References

Baillié, K. & Charnoz, S. 2014, ApJ, 786, 35
Baillié, K., Charnoz, S., & Pantin, E. 2015, A&A, 577, A65
Baruteau, C. & Masset, F. 2008, ApJ, 672, 1054
Bitsch, B. & Kley, W. 2011, A&A, 536, A77
Bitsch, B., Morbidelli, A., Lega, E., & Crida, A. 2014, A&A, 564, A135
Goldreich, P. & Tremaine, S. 1979, ApJ, 233, 857
Goldreich, P. & Tremaine, S. 1980, ApJ, 241, 425
Helling, C., Winters, J. M., & Sedlmayr, E. 2000, A&A, 358, 651
Lynden-Bell, D. & Pringle, J. E. 1974, MNRAS, 168, 603
Paardekooper, S.-J., Baruteau, C., & Kley, W. 2011, MNRAS, 410, 293
Paardekooper, S.-J. & Papaloizou, J. C. B. 2008, A&A, 485, 877
Paardekooper, S.-J. & Papaloizou, J. C. B. 2009a, MNRAS, 394, 2283
Paardekooper, S.-J. & Papaloizou, J. C. B. 2009b, MNRAS, 394, 2297
Semenov, D., Henning, T., Helling, C., Ilgner, M., & Sedlmayr, E. 2003, A&A, 410, 611
Shakura, N. I. & Sunyaev, R. A. 1973, A&A, 24, 337
Tanaka, H., Takeuchi, T., & Ward, W. R. 2002, ApJ, 565, 1257
Ward, W. R. 1991, in Lunar and Planetary Science Conference, Vol. 22, Lunar and Planetary Science Conference, 1463